

SUPPORTING INFORMATION FOR:

Aqueous Self-Assembly of Hydrophobic Macromolecules with Adjustable Backbone Rigidity

Guangzhou, ‡^a Dapeng Liu, ‡^b Jiaping Lin*^a, Xiaosong Wang*^b

Table S1 The repulsive parameter (a_{ij}) and the chain stiffness potential (k_c) of PFpP as a function of temperature.

Temperature	25 °C	40 °C	60 °C	70 °C
The repulsive parameters a_{ij}	$a_{RO} = a_{RP} = 60,$ $a_{RS} = 70$	$a_{RO} = a_{RP} = 50,$ $a_{RS} = 60$	$a_{RO} = a_{RP} = 40,$ $a_{RS} = 50$	$a_{RO} = a_{RP} = a_{RS} =$ 30
The chain stiffness potential k_c	$k_c = 5k_B T$	$k_c = 2k_B T$	$k_c = 0k_B T$	$k_c = 0k_B T$
Simulated morphologies	Nanosheet	Nanovesicle	Irregular nanoparticle	Worm-like nanostructure

(Note: 1. R, O, P and S denotes to benzyl/Cp, COFeCO, $(CH_2)_3P$ groups and solvents; 2. k_B is the Boltzmann constant and T is temperature)

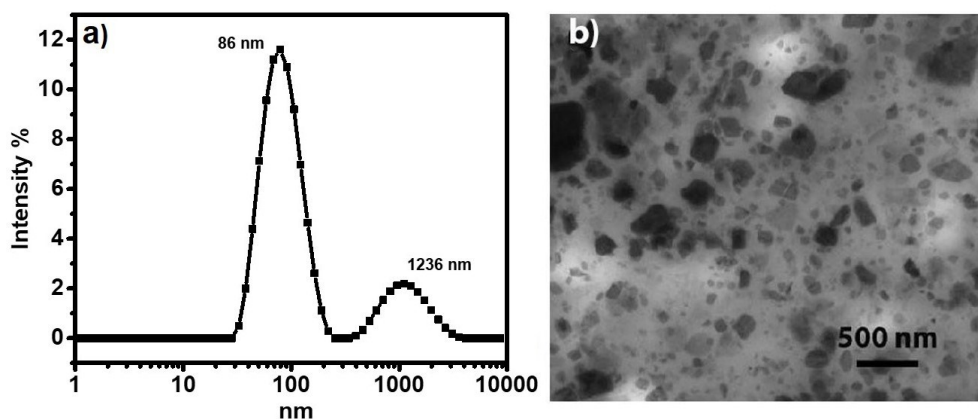


Figure S1. a) DLS profile and b) TEM images for the $P(FpC_3P)_7$ aggregates prepared at 25 °C.

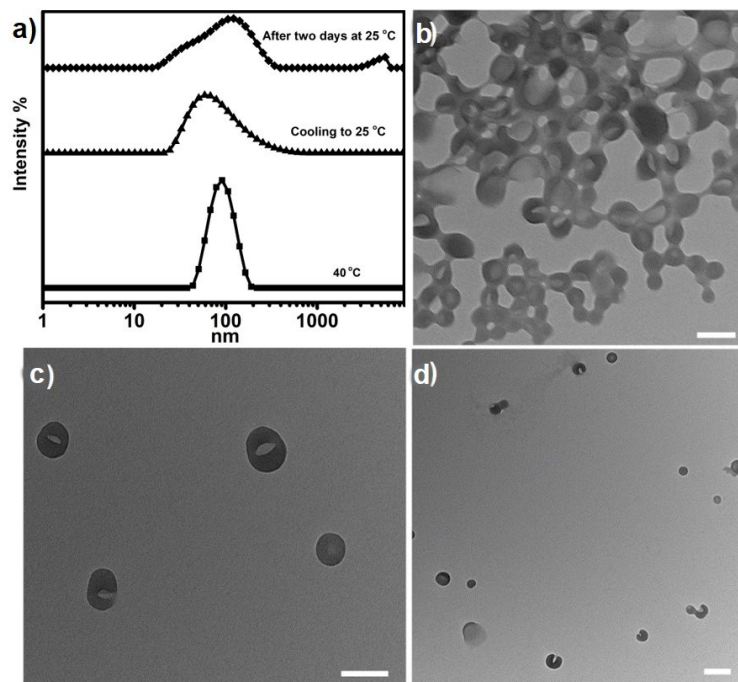


Figure S2. a) DLS profile and TEM images for P(FpC₃P)₇ nanovesicles in DMSO/water (1/9 v/v) prepared at 40 °C. (the TEM grid was prepared after the solution cooling to 25 °C. Scale bar = 100 nm

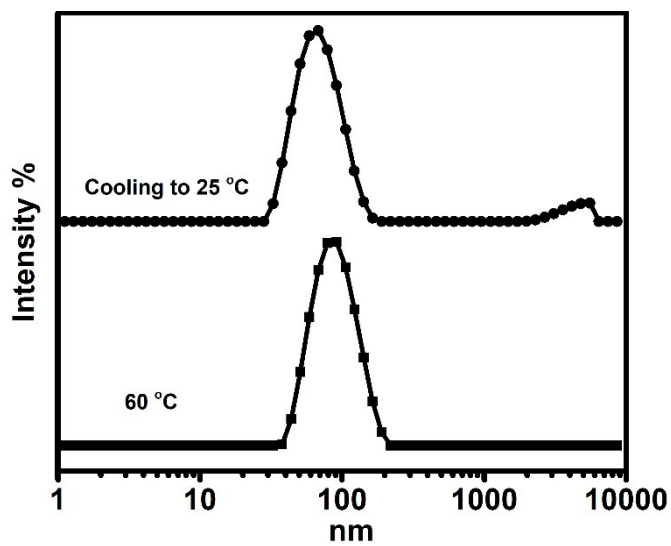


Figure S3. DLS profiles for P(FpC₃P)₇ irregular aggregates in DMSO/water (1/9 v/v) formed at 60 °C and the solution after cooling to 25 °C.

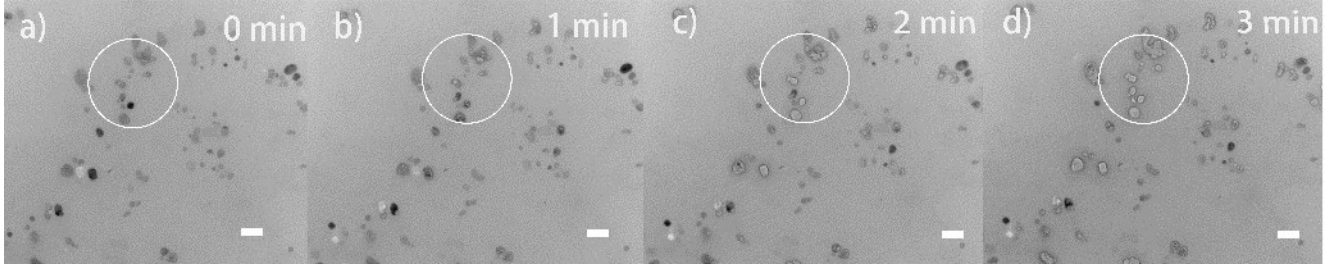


Figure S4 TEM images for the irregular P(FpC₃P)₇ aggregates with different exposure time to the electron beam. Scale bar = 100 nm

1. Simulation

1.1 Dissipative Particle Dynamic (DPD) simulation method

Dissipative particle dynamics (DPD) is a mesoscopic simulation method originated by Hoogerbrugge and Koelman^{S1,S2} and developed by Robert and Patrick.^{S3} In this method, several neighboring molecules are coarse-grained into a single particle. Newton's equations of motion are applied to calculate the trajectories of beads in the system. A modified velocity-Verlet algorithm is used for the propagation of the positions and velocities of the beads.

According to the DPD method the force \mathbf{F}_i acting on a coarse-grained DPD bead i is the sum of the conservative force, dissipative force, and random force, represented as the following equation:

$$\mathbf{F}_i = \sum_{i \neq j} (\mathbf{F}_{ij}^C + \mathbf{F}_{ij}^D + \mathbf{F}_{ij}^R) \quad (\text{S1})$$

The three kinds of forces on the right side of the above equation take the following forms:

$$\mathbf{F}_{ij}^C = \begin{cases} a_{ij} (1 - r_{ij} / r_c) \hat{\mathbf{r}}_{ij} & r_{ij} < r_c \\ 0 & r_{ij} \geq r_c \end{cases} \quad (\text{S2})$$

$$\mathbf{F}_{ij}^D = \begin{cases} -\gamma (1 - r_{ij} / r_c)^2 (\hat{\mathbf{r}}_{ij} \cdot \mathbf{v}_{ij}) \hat{\mathbf{r}}_{ij} & r_{ij} < r_c \\ 0 & r_{ij} \geq r_c \end{cases} \quad (\text{S3})$$

$$\mathbf{F}_{ij}^R = \begin{cases} (2\gamma k_B T)^{1/2} (1 - r_{ij} / r_c) \theta_{ij} (dt)^{-1/2} \hat{\mathbf{r}}_{ij} & r_{ij} < r_c \\ 0 & r_{ij} \geq r_c \end{cases} \quad (\text{S4})$$

a_{ij} is the repulsive parameter between two arbitrary beads i and j , r_{ij} is the distance between these two beads $r_{ij} = |\mathbf{r}_i - \mathbf{r}_j|$, and $\hat{\mathbf{r}}_{ij}$ is the unit vector $\hat{\mathbf{r}}_{ij} = (\mathbf{r}_i - \mathbf{r}_j) / r_{ij}$. r_c is the cutoff distance. γ is the strength of the dissipation between bead i, j . According to our previous work, the friction factor γ was set to 4.5^{S4,S5}. $\mathbf{v}_{ij} = \mathbf{v}_i - \mathbf{v}_j$. θ_{ij} is a random fluctuating variable with Gaussian statistics and has zero mean and unit deviation.

For diblock copolymers, an additional harmonic spring potential $U_{ij}^s = \frac{1}{2} k_s (r_{ij} - r_0)^2$ is applied on each pair of two bonded

beads i and j , and the chain stiffness potential $U_{ijk}^c = \frac{1}{2} k_c (\cos(\theta) - \cos(\theta_0))^2$ is performed on three neighboring beads i, j

and k in rod blocks.

1.2 π - π stack conjugate potential

In DPD method, the conservative potential (Equation S2) provides a repulsive force between the interacted particles. However, there are high densities of benzyl and Cp (denoted by R) groups along the polymer chains. The interactions among these groups are p-p stack conjugation. Accordingly, the traditional repulsive force in DPD method is insufficient to simulate the conjugation among R groups. In addition to the potentials in DPD method, an attractive potential should be applied for providing this conjugation. In present work, we adopted the attractive potential as follows^{S6}:

$$U_{ij}^\pi = -k_\pi \cos^2 \left[\pi (r - r_c) / 2 / (r_{\text{ext}} - r_c) \right] \quad r_c \leq r \leq r_{\text{ext}} \quad (\text{S5})$$

where k_π is the strength of the potential, r_c is the lower cutoff distance, which equals to the r_c in DPD method and r_{ext} is the upper cutoff distance. This potential is firstly proposed by Cooke *et al.*, which has been adopted to simulate the layer structure formed by phospholipids.

1.3 Parameter setting

Repulsive parameter. In the DPD method, there is a linear relationship between the Flory-Huggins parameter χ_{ij} and interaction parameters a_{ij} .^{S3} Larger χ_{ij} means larger a_{ij} . For beads of the same species, the repulsive parameters a_{ij} were set to 25. Since the COFeCO and $(\text{CH}_2)_3\text{P}$ groups are hydrophilic (hydrogen bonding can be formed among these groups and water), while the benzyl and Cp groups are hydrophobic, we set $a_{\text{OP}} = a_{\text{OS}} = a_{\text{PS}} = 25$, $a_{\text{RO}} = a_{\text{RP}} = 60$, $a_{\text{RS}} = 75$ at 25 °C, where R, O, P and S denotes to benzyl/Cp, COFeCO, $(\text{CH}_2)_3\text{P}$ groups and solvents, respectively. The values of repulsive parameters a_{RO} , a_{RP} and a_{RS} were varied with temperature. In present work, we used Materials Studio (Blend Module) to calculate the values of χ_{ij} between those groups at different temperatures. The results are shown in Figure S5. It can be seen that the values of χ_{ij} for O-P, O-S and P-S pairs almost remain unchanged with varying temperature. However, for the case of R-O, R-P and R-S pairs, the values of χ_{ij} are linearly decreased with increasing temperature. Accordingly, we set the $a_{\text{RO}} = a_{\text{RP}} = 50$, $a_{\text{RS}} = 60$ at 40 °C, $a_{\text{RO}} = a_{\text{RP}} = 40$, $a_{\text{RS}} = 50$ at 60 °C and $a_{\text{RO}} = a_{\text{RP}} = a_{\text{RS}} = 35$ at 70 °C.

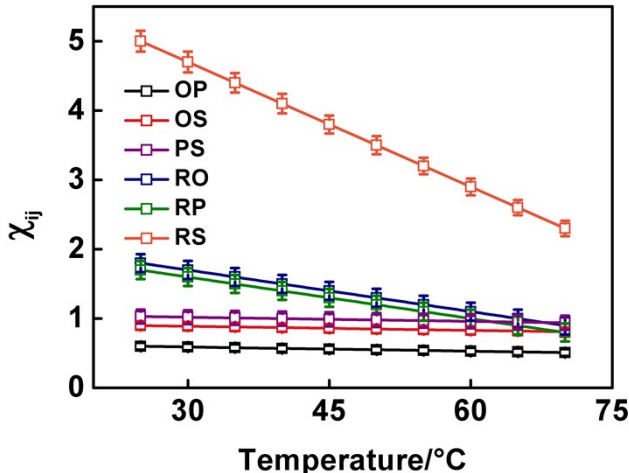


Figure S5. Values of χ_{ij} for the pairs of different species as a function of temperature.

Harmonic spring potential. In this work, the equilibrium bond distance r_0 and were set to be $0.7r_c$. The values of k_s was set as $100k_B T/r_c^2$ (k_B is the Boltzmann constant and T is temperature).^{S7} These values are constant at different temperatures.

Chain stiffness potential. In some cases, the chain conformations may be transformed with temperatures. In the present work, we used Materials Studio to investigate these transformations. The simulation system with one polymer and a certain amount of solvents was constructed using the Amorphous Cell module. Then, using the Discover module, all-atom molecular dynamic simulations were performed under different temperatures. The simulation protocols and the parameters were all chosen according to those in our previous work. With varying the temperature from 25 to 75 °C, the structures of polymers at equilibrium state were obtained after the simulations. Herein, we analyzed the persistence lengths (l_p) of the backbones of these polymers under different temperatures. The formula of l_p is as follows:^{S8}

$$\langle \cos(\theta_i) \rangle = \exp(-l_b / l_p) \quad (\text{S6})$$

θ_i is the angle between two neighboring bonds along the chain. l_b is the average length of all the i bonds. The profile of l_p as a function of k_a is shown as the red profile in Figure S6. The value of l_p is largest at 25 °C, which is approximately 70 nm. When the temperature is lower than 60 °C, with increasing temperature, the value of l_p is decreased almost linearly. For the case of temperature is higher than 60 °C, the value of l_p nearly keeps unchanged at 15 nm. The morphologies of polymers at 25, 50 and 75 °C are provided in the inset of Figure S6. The profile of l_p and morphologies of polymers both represent the evolutionary chain stiffness of polymers with varying temperature.

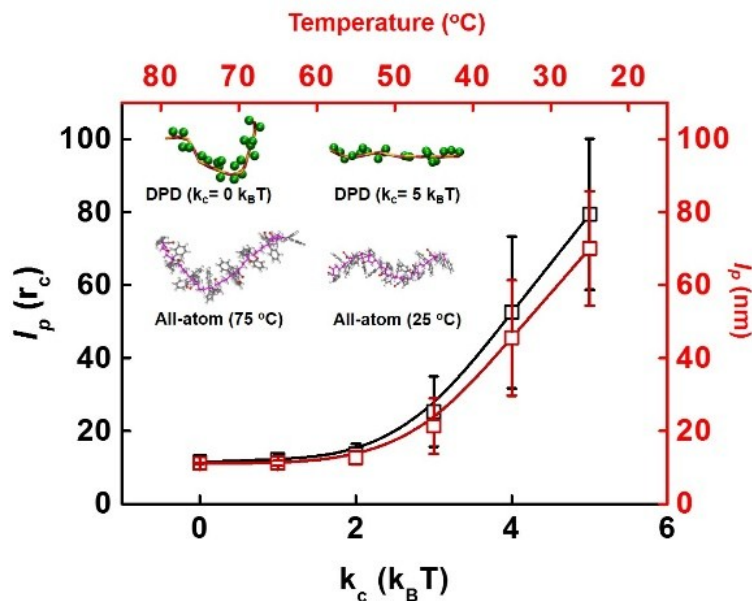


Figure S6. Persistence length as a function of k_c in DPD simulation (the black curve) and temperature in all-atom simulation (the red curve). The chain conformations at 25 and 70 $^{\circ}C$, corresponding to the k_c of 5 $k_B T$ and 0 $k_B T$, are shown in the figure.

In order to denote the transformation of chain stiffness of polymer backbone with changing temperature in our DPD simulations, we reduced the chain stiffness potential k_c from 5 to 0 $k_B T$ as the temperature was increased from 25 to 70 $^{\circ}C$. The equilibrium value of the angle θ_0 was set to be π . A larger value of k_c corresponds to a stronger rigidity of polymer chain. Similar to the case of all-atom simulations, the values of l_p at different temperatures in the DPD simulations were also examined. The statistical result is shown as the black profile in Figure S6. It can be seen that, this profile is extremely close to that obtained from the all-atom simulations. The value of l_p almost keeps $10 r_c$ when k_c is smaller than $2 k_B T$, while it is linearly increased with k_c for the case of $k_c > 2 k_B T$. Accordingly, we can find a quantitative consistent result between the results from all-atom and DPD simulations, indicating the setting values of k_c in the DPD simulations can effectively capture the conformations of polymer backbones under various temperatures. Specifically, the value of k_c was set to 5, 2, 0 and 0 $k_B T$ at 25, 40, 60 and 70 $^{\circ}C$, respectively. The k_c for 60 and 70 $^{\circ}C$ were both set to 0 $k_B T$ because the l_p reaches to the smallest under these two temperatures. For clarity, we provide the a_{ij} and k_c at 25, 40, 60 and 70 $^{\circ}C$ adopted in the present work in Table S1.

REFERENCES

- S1. Hoogerbrugge, P. J.; Koelman, J. M. V. A. *Europhysics letters* **1992**, 19, (3), 155–160.
- S2. Koelman, J. M. V. A.; Hoogerbrugge, P. J. *Europhysics letters* **1993**, 21, (3), 363–368.
- S3. Groot, R. D.; Warren, P. B. *The Journal of chemical physics* **1997**, 107, (11), 4423–4435.
- S4. Jiang, T.; Wang, L.; Lin, S.; Lin, J.; Li, Y. *Langmuir* **2011**, 27 (10), 6440–6448.
- S5. Cai, C.; Wang, L.; Lin, J.; Zhang, X. *Langmuir* **2012**, 28, (9), 4515–4524.
- S6. Cooke, I. R.; Deserno, M. *The Journal of chemical physics* **2005**, 123, (22), 224710.
- S7. Wang, L.; Lin, J.; Zhang, X. *Polymer* **2013**, 54, (14) 3427–3442.
- S8. Doi, M.; Edwards, S. F. *The Theory of Polymer Dynamics*, Clarendon, Oxford, **1986**.